Fluid Inclusion Microthermometry of Imperial Topaz from Capão do Lana Deposit, Ouro Preto, Minas Gerais State, Brazil

ROSA MARIA DA SILVEIRA BELLO[1], KAZUO FUZIKAWA[2], ANTONIO LUCIANO GANDINI[3], JOSÉ VICENTE VALARELLI[1] and DARCY PEDRO SVISERO[1]

[1]Departamento de Mineralogia e Petrologia, Instituto de Geociências/USP, C. P. 11348 – 05422-970 São Paulo, SP, Brazil
[2]Centro de Desenvolvimento da Tecnologia Nuclear/CDTN, C. P. 941 – 30161-970 Belo Horizonte, MG, Brazil
[3]Departamento de Geologia, Escola de Minas/UFOP, Campus Universitário – 35400-000 Ouro Preto, MG, Brazil

Manuscript received May 15, 1995, accepted for publication on November 13, 1995

ABSTRACT

Amongst the many imperial topaz occurrences in the Ouro Preto region, Minas Gerais State, all associated with carbonatic metamorphic rocks of the Minas Supergroup, the Capão do Lana deposit has been selected for a fluid inclusion study. Topaz crystals of this deposit always contain abundant fluid inclusions of variable morphology and distribution, with saline aquo-carbonic composition. Microthermometric data indicated three groups of samples with different densities and phase ratios as follows:

Groups	Average CO_2 density (g/cc)	Range of total fluid density g/cc
1	0.8648	0.9297–0.9747
2	0.8466	0.9400–0.9866
3	0.7559	0.9620–1.0288

In the crystals of the same group, the total homogenization occurred either as H_2O or CO_2 phases indicating trapping of two originally immiscible fluids. The trapping temperature and pressure obtained for all groups (275 to 300°C and 1.75 to 3.2kbar) and the equilibrium reaction curves involving solid inclusions present in the crystals indicate a hydrothermal post-metamorphic origin for the imperial topaz in this deposit.

Key words: fluid inclusions, microthermometry, geothermometer, imperial topaz.

INTRODUCTION

There are several imperial topaz occurrences at southwest of Ouro Preto city in Minas Gerais State. Some of the most important are the Vermelhão deposit (Saramenha Hill), those located near the Dom Bosco region (Caxambu, the Capão do Lana, and the Bela Vista deposits) and the Boa Vista deposit, located near the town of same name. Northeast of Ouro Preto is the Antonio Pereira deposit (Fig. 1).

The occurrences are all distributed along the Dom Bosco syncline, except the Antonio Pereira

Correspondence to: Rosa Maria da Silveira Bello or José Vicente Valarelli (at the above address).

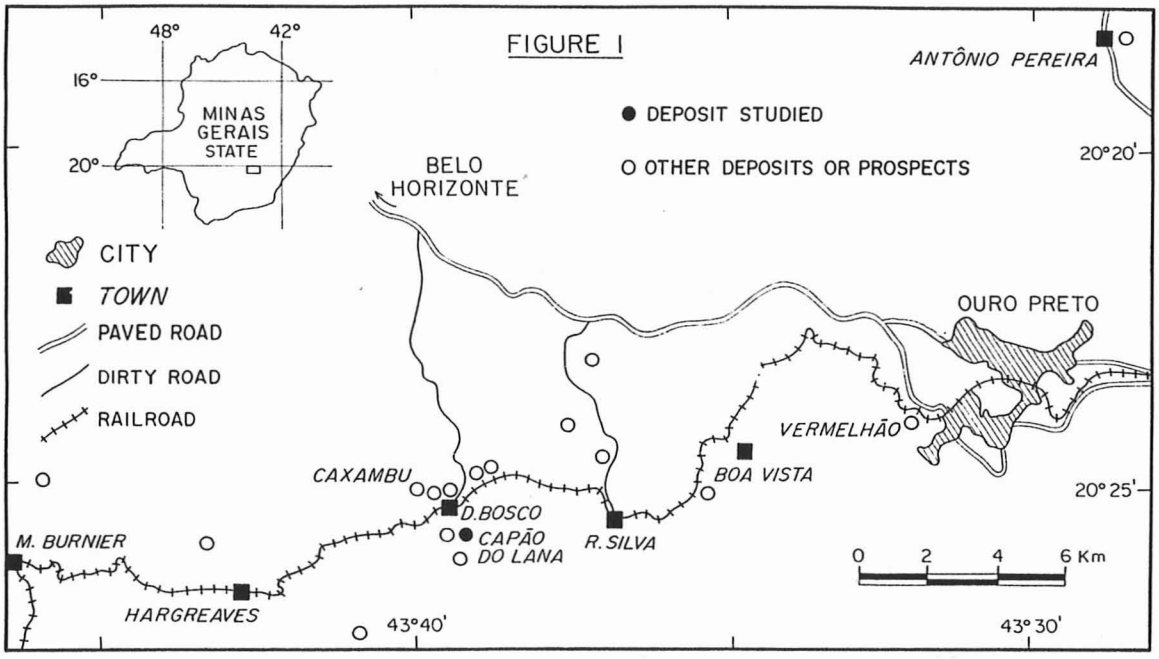

Fig. 1 — Location of the main imperial topaz deposits and prospects in the Ouro Preto region, Minas Gerais State (modified from Gandini *et al.*, 1991).

deposit, which is located in the Mariana anticline. The mineralization is controlled by normal faults cross-cutting carbonatic metamorphic rocks of the Minas Supergroup.

It should be pointed out that this gemmological variety of topaz, characterized essentially by its orange yellowish colour, is relatively rare, being known in Brazil only near Ouro Preto. Other occurrences are found in Siberia, where the deposits are almost completely exhausted, and in Pakistan (Gübelin *et al.*, 1986).

The imperial topaz occurrences of Ouro Preto are known since last century (Gorceix, 1881). Due to their rarity and importance as a gemstone they have been subject of numerous mineralogical and geological studies (Olsen, 1971; Petrov *et al.*, 1977; Pires, 1983; Ferreira, 1983, 1987, 1991 and Cassedanne, 1989, among others). Studies dealing with detailed mineralogical data, including fluid inclusion microthermometry, have also been conducted in some deposits (Gandini *et al.*, 1991; Gandini *et al.*, 1992a; Gandini *et al.*, 1992b; Gandini, 1994 and Bello *et al.*, 1995).

Despite the previous work, a number of problems remain unsolved, especially those related to the genesis of the mineralization. The available interpretations on the origin of topaz in these occurrences are conflicting and more detailed studies on the characteristics of these deposits are necessary.

The results of detailed fluid inclusions studies in topaz crystals from Capão do Lana deposit are presented here. The studies aimed to characterize the mineralizing solution as well as to determine the possible temperature and pressure conditions during the topaz crystallization.

The fluid inclusion study was carried out on a Chaixmeca microthermometry stage (Poty *et al.*, 1976), in the Fluid Inclusions Laboratory at the Instituto de Geociências, Universidade de São Paulo. Some of the data were obtained in the Centro de Desenvolvimento de Tecnologia Nuclear from Comissão Nacional de Energia Nuclear (CDTN/CNEN), in Belo Horizonte.

GEOLOGY OF THE CAPÃO DO LANA MINE AREA

The imperial topaz occurrences in the Ouro Preto region are related to the Minas Supergroup rocks, being controlled by specific structures and lithologies. The mineralization is associated with

normal faults, which cross-cut the Minas Supergroup metamorphic rocks striking predominantly N60°W. These fault zones are attributed to a Cretaceous or Terciary tectonic event (D_5) in the area (Alkmin *et al.*, s.d. and Marshak & Alkmin, 1989). These authors also characterized four major tectonic events in the region (D_1 – contraction; D_2 – contraction; D_3 – extension and D_4 – compression), showing that D_5 reactivated structures formed in the previous events. Ferreira (1983, 1991) concluded that the last tectonic event in the region is related to the appearance of several syntectonic volcanic spots which would have originated non-metamorphosed, silica saturated rocks.

In the Capão do Lana mine area the metamorphic rocks consist of phyllites, quartzites and dolomites of the Piracicaba Group (Ferreira, 1991). There is a brecciated zone formed by a vertical fault striking N60°W which cross-cuts the phyllites and the dolomitic marbles, where veins (generally a few centimeters thick) and "buchos" (tens of centimeters) containing topaz, quartz, kaolinite, pyrophyllite, (± hematite, rutile and euclase) are observed. This zone is known as the mineralized zone (Ferreira, 1991).

The metamorphic rocks and veins are deeply weathered preserving only some of the old structures and primary minerals such as quartz, hematite, topaz, pyrophyllite, rutile, euclase and sericite. The topaz is usually found in kaolin masses and in carbonatic weathered products.

Based on localized studies, some authors suggest that the mineralization was originated either during a pneumatolithic/hydrothermal activity related to a pre-metamorphic stage (Olsen, 1971), or during the low grade metamorphic peak which characterizes the Minas Supergroup rocks (Pires, 1983). On the other hand, studies on different occurrences (Ferreira, 1983) indicate that the mineralized veins are intimately associated with dolomitic rocks, and that the topaz may have been generated by hydrothermal activity related to the final stage of the last volcanic event in the region, which occurred during the late Cretaceous or early Terciary.

CHARACTERIZATION OF TOPAZES AND FLUID INCLUSIONS

Topaz occurs mostly as terminated prismatic crystals 1 to 4cm long (studied samples) commonly presenting colours varying from yellow to orange. They usually contain a few types of crystalline inclusions such as dolomite, hematite, goethite, topaz, rutile, quartz, kaolinite and pyrophyllite (Ferreira, 1983, 1991 and Pires, 1983). In addition, Gandini *et al.* (1992a) and Gandini (1994) determined the presence of needdle shapped inclusions of tremolite.

In all samples, a large number of two-phase fluid inclusions were observed at room temperature (25°C). They are comprised of saline aqueous solutions and CO_2, with variable morphology and orientation in the host. As discussed in Gandini *et al.* (1991) and Gandini (1994), the fluid inclusions show both regular and irregular contours. The regular shaped inclusions are elongated, sometimes forming tiny tubes.

The fluid inclusions show extremely variable sizes (4μm to 460μm). For microthermometric determinations, only those between 15 and 50μm (length of the longest axis) have been considered, because the larger ones may decrepitate or leak during heating.

Fluid inclusions with features indicating leakage and necking down are also commonly present. Careful microscopy allowed their exclusion from the microthermometric study.

MICROTHERMOMETRY

The fluid inclusions in the Capão do Lana topaz were classified in four distinct types by Gandini *et al.* (1991), according to their orientation relative to the host crystal. They are: *type a* – fluid inclusions located parallel to the topaz crystal *c*-axis presenting both regular and irregular contours; *type b* – fluid inclusions located in non-parallel arrangement to the *c*-axis, also exhibiting regular and irregular contours; *type c* – fluid inclusions with irregular contours randomly distributed in the crystal; and *type d* – fluid inclusions present in healed fractures of the crystal. Following this classification, the microthermometric determinations al-

lowed to distinguish three distinct groups of samples independent of the four types of inclusions discussed above. The results of these determinations are presented in tables I, II and III.

CO_2 HOMOGENIZATION TEMPERATURES (Th_{CO_2})

These temperatures vary largely independent of the dimensions and mode of occurrence of the inclusions. The variations are similar in all types of inclusions as shown in figure 2 and table I.

In all samples, the homogenization always occurred to liquid phase. Assuming that the carbonic phase has a small presence of other volatile compounds, the most frequent values of Th_{CO_2} allowed the calculation of the CO_2 average densities, according to P-V-T-X experimental data for pure systems from the literature (Roedder, 1984; Nicholls & Crawford, 1985, among others).

The microthermometric study indicated that the four types of fluid inclusions from each sample presented a similar behavior. Nevertheless, the comparison of each type of fluid inclusion in the various samples, shows differences mainly regarding to the Th_{CO_2} and the volume of carbonic phase in the inclusion (V_{CO_2}/V_{tot}). According to these parameters, three distinct groups of samples were identified, each having the four types of inclusions with similar Th_{CO_2} and V_{CO_2}/V_{tot} values. Overall, the different types of inclusions show the same Th_{CO_2} interval (8.0-23.2°C), also exhibiting some coincidences in the higher frequency temperature ranges (Fig. 2). Each one of these temperature ranges is representative of a specific group of crystal samples. Therefore, in the *type a* inclusions three ranges of temperatures with higher measurement frequencies can be indicated: the first, between 9.6 and 11.2°C corresponding to *Group 1*; and the second, between 11.2 and 12.8°C corresponding to *Group 2*. Because of the overlap of measurements in these two groups, the calculated average CO_2 densities varied from 0.8619 to 0.8476g/cc. The third range of temperatures

TABLE I

Microthermometric data relative to fluid inclusion of types a, b, c, and d, for the three groups of samples.

Gr	T	Range of Th_{CO_2} (°C)	Range of V_{CO_2}/V_{tot} (%)	Range of Tf_{CO_2} (°C)	TmCl (°C)		Range of Th_{CO_2} (°C)	Th_{tot} Range of major frequency (°C)
					Range	Average		
1	a	8,8 to 11,2	45 to 60	-57,0 to -56,6	5 to 8	5,6/7,0	230 to 310	290 to 300 (crít.)
	b	8,8 to 10,4	35 to 60	-56,8 to -56,6	6 to 9	7,3	280 to 300	290 to 300 (crít.)
	c	8,8 to 10,4	40 to 60	-57,4 to -57,2	7 to 8	7,5	230 to 300	290 to 300 (CO_2)
	d	8,0 to 10,4	40 to 60	-58,2 to -57,0	5 to 8	6,1/7,3	290 to 320	300 to 310 (crít.)
2	a	10,4 to 12,8	30 to 50	-57,0 to -56,6	6 to 8	6,4/7,7	260 to 300	270 to 300 (H_2O, crít., CO_2)
	b	12,0 to 12,8	30 to 50	-57,2 to -56,6	6 to 8	6,8	—	—
	c	11,2 to 14,4	30 to 40	-57,2 to -56,8	6 to 8	7,0	—	—
	d	11,2 to 12,8	30 to 50	-56,8 to -56,6	6 to 8	7,1/7,5	290 to 300	290 to 300 (crít.)
3	a	21,6 to 22,4	10 to 20	-57,2 to -56,6	5 to 7	5,6/6,4	280 to 290	280 to 290 (H_2O)
	b	20,8 to 23,2	10 to 30	-57,8 to -56,8	5 to 7	5,7/5,9	270 to 290	280 to 290 (H_2O)
	c	20,8 to 22,4	10 to 30	-56,8 to -56,6	5 to 7	6,0	280 to 290	280 to 290 (H_2O, CO_2)
	d	20,8 to 22,4	10 to 30	-57,8 to -56,6	4 to 7	5,2/5,6	290 to 300	290 to 300 (H_2O)

Gr: group of samples; T: type of fluid inclusion; Th_{CO_2} : homogenization temperature of the CO_2 phase: V_{CO_2}/V_{tot} : volume of the CO_2 phase in fluid inclusions; TmCl: clathrate melting temperature; Th_{tot}: temperature of total homogenization.

TABLE II
Parameters calculated from Table I data.

Gr	T	d_{CO_2} (g/cc)	d_{H_2O} (g/cc)	d_{total} (range) (g/cc)	salinity (wt% NaCl equiv.)	compositions (range)		
						X_{H_2O}	X_{NaCl}	X_{CO_2}
1	a	0,8619	1,0463	0,9322/0,9680	5,77 to 8,13	0,6417 to 0,7553	0,0121 to 0,0206	0,3462 to 0,2240
	b	0,8648	1,0339	0,9325/0,9747	5,23	0,6420 to 0,8257	0,0109 to 0,0141	0,3470 to 0,1602
	c	0,8619	1,0313	0,9297/0,9635	4,87	0,6436 to 0,7969	0,0102 to 0,0126	0,3463 to 0,1906
	d	0,8655	1,0411	0,9356/0,9717	5,23 to 7,31	0,6368 to 0,7932	0,0117 to 0,0184	0,3481 to 0,1908
2	a	0,8476	1,0385	0,9361/0,9866	4,51 to 6,81	0,7268 to 0,8585	0,0107 to 0,0192	0,2582 to 0,1290
	b	0,8435	1,0403	0,9419/0,9812	6,12	0,7286 to 0,8539	0,0146 to 0,0171	0,2568 to 0,1290
	c	0,8387	1,0377	0,9581/0,9780	5,77	0,7986 to 0,8555	0,0151 to 0,0161	1,1864 to 0,1283
	d	0,8463	1,0339	0,9400/0,9786	4,87 to 5,59	0,7304 to 0,8554	0,0115 to 0,0156	0,2581 to 0,1290
3	a	0,7518	1,0494	0,9865/1,0235	6,81 to 7,79	0,9044 to 0,9456	0,0241 to 0,0251	0,0715 to 0,0331
	b	0,7536	1,0525	0,9625/1,0235	7,64 to 7,97	0,8605 to 0,9418	0,0220 to 0,0251	0,1170 to 0,0331
	c	0,7565	1,0501	0,9620/1,0208	7,48	0,8613 to 0,9432	0,0215 to 0,0235	0,1172 to 0,0333
	d	0,7559	1,0572	0,9664/1,0288	8,13 to 8,77	0,8580 to 0,9409	0,0234 to 0,0278	0,1177 to 0,0331

Gr: group of samples; T: type of fluid inclusions; d_{CO_2}: density of CO_2 – rich phase; d_{H2O}: density of H_2O – rich phase; d_{total}: bulk density.

(*Group 3*) was well different from the previous ones, varying between 21.6 and 22.4°C and having an average CO_2 density of 0.7559g/cc.

In the *type b* inclusions (Fig. 2), the three ranges of Th_{CO_2} and their respective frequencies are better defined and placed at 8.8-10.4°C (*Group 1*), 12.0-12.8°C (*Group 2*) and 20.8-23.2°C (*Group 3*) corresponding to average densities of 0.8648g/cc, 0.8435g/cc and 0.7536g/cc, respectively.

In the histogram referent to the *type c* inclusions, the sequence of Th_{CO_2} intervals and their respective average densities for the three groups of samples are: 8.8-10.4°C and 0.8619g/cc (*Group 1*); 12.8-14.4°C and 0.8387g/cc (*Group 2*); 20.8-22.4°C and 0.7565g/cc (*Group 3*).

Finally, in the *type d* inclusions (Fig. 2), the variation of Th_{CO_2} and the average densities values for the three groups are respectively: *Group 1* – from 8.0 to 10.4°C and 0.8655g/cc; *Group 2* – from 11.2 to 12.8° and 0.8463g/cc; *Group 3* – from 20.8 to 22.4°C and 0.7559g/cc.

Due to the coincidence of the Th_{CO_2} intervals for the different types of inclusions, the obtained

TABLE III
Salinity variations (wt% NaCl equiv.) in all inclusion types from distinct sample groups.

	type a	type b	type c	type d	range
Group 1	7,0	5,2	4,9	6,2	4,9 to 7,0
Group 2	5,9	6,1	5,8	5,2	5,2 to 6,1
Group 3	7,4	7,8	7,5	8,5	7,4 to 8,5
range	5,9 to 7,4	5,2 to 7,8	4,9 to 7,5	5,2 to 8,5	

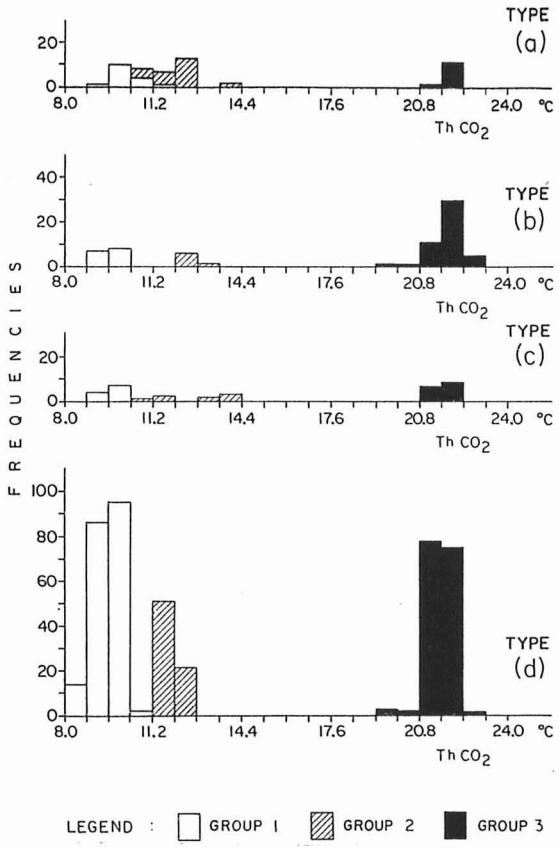

Fig. 2 — CO_2 homogenization temperature frequency histogram for the different fluid inclusion types: (a) *type a* – inclusions parallel to the topaz *c*-axis; (b) *type b* – inclusions inclined to the topaz *c*-axis; (c) *type c* – inclusions randomly distributed in the crystals; (d) *type d* – inclusions in internal healed fractures.

CO_2 average densities were similar, independent of the mode of occurrence. It should be noted that the *type d* inclusions are related to healed fractures which do not extend up to the boundary of crystals indicating a pseudosecondary origin.

The different groups of samples, which are characterized by the CO_2 densities of their fluid inclusion (d_{CO_2}, in Tab. II), may suggest trapping in more than one stage, possibly under different pressure and temperature conditions. Nevertheless, this interpretation is limited by lack of satisfactory field relations, as "in situ" sampling was not possible in this case. The samples, collected from the conveyor belt after hydraulic mining and washing, were supplied by TIMCIL (Topázio Imperial Mineração, Comércio e Indústria Ltda).

CO_2 Melting Temperature (Tm_{CO_2})

All types of inclusions (a, b, c, and d) present in the three groups of samples show a roughly similar range of Tm_{CO_2} values, (concentrated between –57.0 and –56.6°C), indicating a high purity of the CO_2 phase (CO_2 triple point = – 56.6°C). The small variations towards lower temperatures (Fig. 3) indicate the presence of other components dissolved in the carbonic phase. It is not possible to identify these components by microthermometric investigation, but they are usually CH_4, N_2 or other hydrocarbons (Roedder, 1984). In fact, Gandini *et al.* (1992b) and Gandini (1994), using infrared absorption spectroscopy, concluded that hydrocarbons (probably CH_4) occur associated with CO_2 in some inclusions, while the laser Raman spectroscopy indicated a possible presence of N_2.

The microthermometric data are not similar for each type of inclusion belonging to different samples and sometimes not even in the same sample. These data and the variations in the amount of compounds observed in the spectroscopic analysis (Gandini *et al.*, 1992b; Gandini, 1994), suggest local differences in the composition of the mineralizing fluids.

Salinity

All inclusions contain clathrate compounds ($CO_2.5.75H_2O$). This increases the salinity of the remaining aqueous fluid because the water molecules are incorporated into these compounds. Therefore, the true salinity of aqueous solution cannot be determined using ice melting temperatures. So clathrate melting temperatures (Tm_{Cl}) should be used for this purpose (Collins, 1979; Roedder, 1984; Fuzikawa, 1985).

The microthermometric determinations indicated that in each group of samples the four types of inclusions presented a similar range of clathrate melting temperatures (Tab. I). This indicated that the salinities were only slightly different, independent of the characteristics of these inclusions.

Figure 4 shows the Tm_{Cl} histogram for the three groups of samples. Considering only the

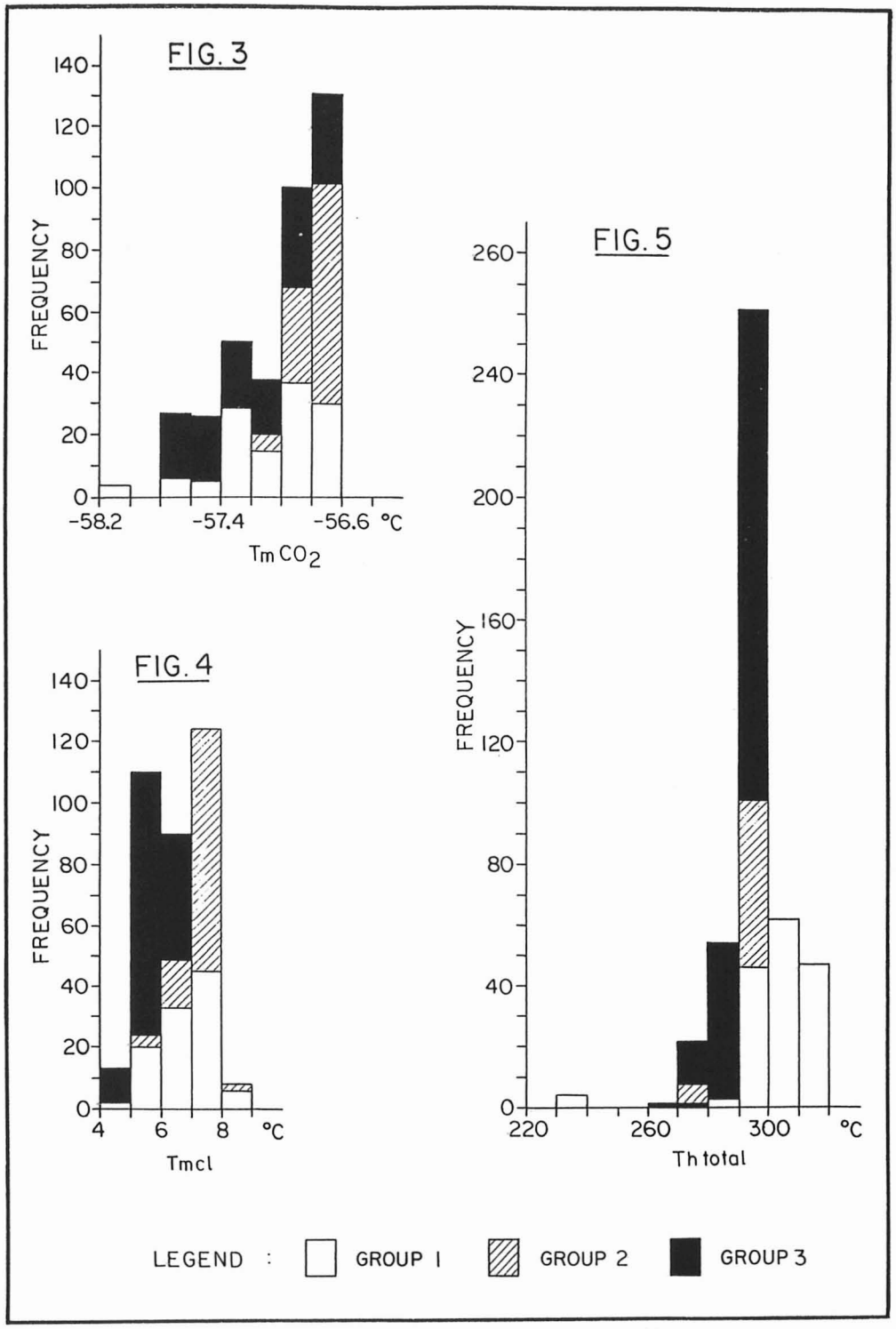

Fig. 3 — CO_2 melting temperature frequency histogram for all three groups of samples. Fig. 4 — Clathrate compound melting temperature frequency histogram for all three groups of samples. Fig. 5 — Histogram showing the frequency of total homogenization temperature in fluid inclusions of the three groups of samples.

peaks corresponding to Tm_{Cl} major frequencies in each group, and using the experimental data for the system CO_2-H_2O-NaCl (Nicholls & Crawford, 1985 and the figure 2 from Collins, 1979), the following salinities for the aqueous solutions were determined (Tab. II):

a) *Group 1* samples: Tm_{Cl} major frequency between 5.0 and 8.0°C, with average values between 5.6 and 7.5°C, and salinities varying from 4.87 to 8.13wt% NaCl equivalent.

b) *Group 2* samples: Tm_{Cl} major frequency between 6.0 and 8.0°C, with average from 6.4 to 7.7°C and salinities varying from 4.51 to 6.81wt% NaCl equivalent.

c) *Group 3* samples: Tm_{Cl} major frequency between 5.0 and 7.0°C, with average from 5.2 to 6.4°C and salinities varying from 6.51 to 8.77wt% NaCl equivalent.

There are differences in the Tm_{Cl} variation range, and consequently in the corresponding salinities for each type of inclusion, when the three groups of samples are considered separately, or even in different types of inclusions from the same group. So, to verify a possible trend in these variations, the average salinities were calculated from the average Tm_{Cl} for all inclusions of each type within a specific group (Tab. III).

The values shown in tables II and III indicate that, in most cases, differences in salinity are small within each group and even among the different groups, although there is a slight tendency to higher values in the fluids of *Group 3* inclusions. These differences, may provide additional evidence for local heterogeneities in the solution composition.

Temperatures of Total Homogenization (Th_{tot})

Although the Th_{tot} was reasonably similar for all types of fluid inclusions, there are some small variations as seen in figure 5. The range of Th_{tot} variations are narrow and similar in each group. There is a larger dispersion only for *Group 1* where Th_{tot} vary between 230 and 320°C, with maximum concentration between 290 and 320°C. In *Group 2*, the temperatures vary from 260 to 300°C with maximum concentration between 290 and 300°C, and in *Group 3* from 270 to 300°C with maximum concentration between 290 and 300°C.

In *Group 1* samples, the higher frequency is concentrated towards higher Th_{tots}. This is due to the influence of *type d* inclusions which show Th_{tot} slightly higher than *type a, b,* and *c* (Tab. I). Furthermore, it is also evident in table I that the Th_{tots} for *Group 1* inclusions are higher than for other groups, indicating small differences in the trapping conditions of the three groups.

It was observed that in crystals from the same group, sometimes in a single sample, the fluid inclusions presented small variations of V_{CO_2}/V_{tot}, which suggest three possible homogenization behaviours: expansion of the CO_2 phase, contraction of the CO_2 phase or critical homogenization. Even considering these different behaviours, inclusions in samples of different groups show some well defined tendencies: in *Group 1*, where the V_{CO_2}/V_{tot} most frequent ratios were between 45 and 60%, the homogenization was predominantly critical, and in a few cases, the expansion of the CO_2 phase also occurred; in *Group 2* (V_{CO_2}/V_{tot} = 30 to 50%) the three types of homogenization were observed; and in *Group 3* (V_{CO_2}/V_{tot}) = 10 to 30%) the homogenization occurred predominantly by contraction of the CO_2 phase, although in a few cases expansion of CO_2 was also observed.

These results suggest trapping of H_2O-CO_2 fluids in state of immiscibility near the critical composition. In these conditions, and when a large number of measurements are available, Roedder's (1984) indicates the lowest Th_{tot} values as representative of the true temperatures of formation, reflecting trapping directly on the solvus of the system. Therefore, the results in table I and figure 5 indicate that inclusions of *Groups 1* and *2* were trapped at temperatures around 290-300°C, while the trapping of *Group 3* fluid inclusions occurred between 275 and 285°C.

ISOCHORES

The Th_{CO_2}, Tm_{Cl} and V_{CO_2}/V_{tot} data (Tab. I) were used to calculate both the molar fractions of the components (X_{H_2O}, X_{NaCl} and X_{CO_2}) and the bulk density (d_{total}) of the fluid inclusions (Tab. II), as well as to construct their respective isochores (Fig. 6). These parameters were calculated by the equations of state for the H_2O-NaCl-CO_2 system, given by Nicholls & Crawford (1985).

For each type of inclusion in the different groups, the average values from the higher Th_{CO_2} frequencies were considered. They were associated with their corresponding Tm_{Cl} and V_{CO_2}/V_{tot} variations. In table II, the range of variations of total densities and variations within each group and

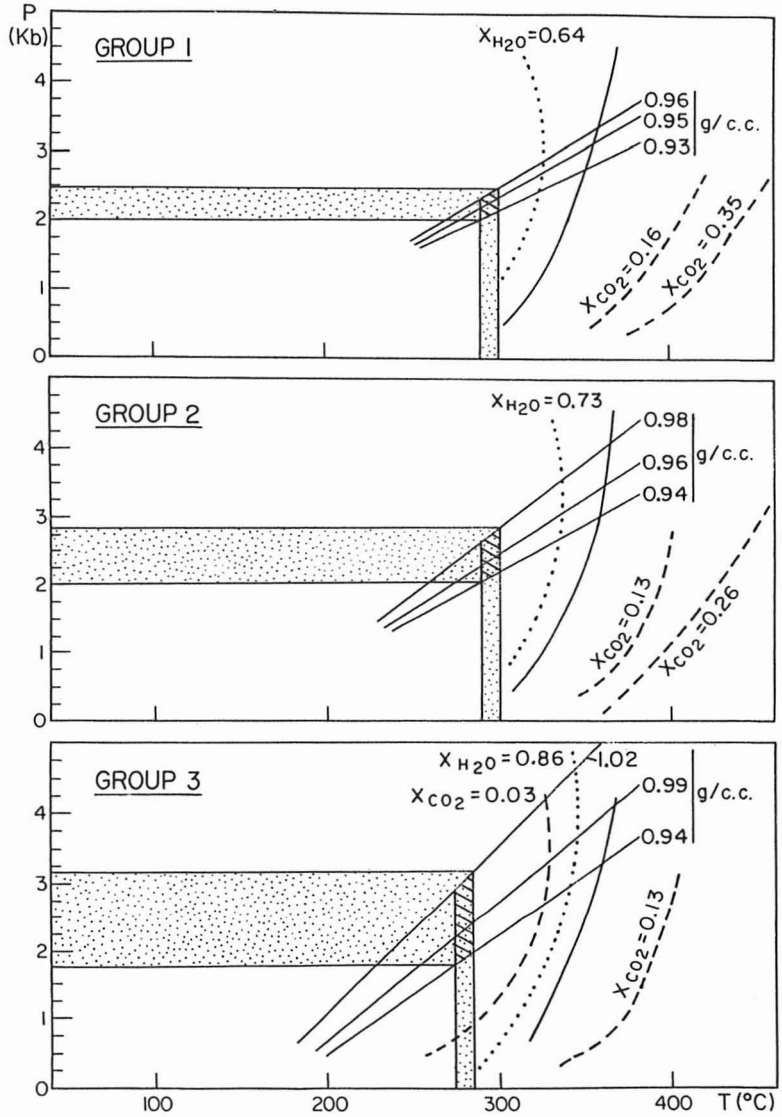

Fig. 6 — P *vs.* T diagrams showing the range of true inclusion trapping conditions and the reaction equilibrium curves: 5 dolomite + quartz + H_2O = tremolite + 3 calcite + 7 CO_2 (data from Skippen, 1974) referent to X_{CO_2} limit values in each group of samples (dashed lines); and kaolinite + 2 quartz = pyrophyllite + H_2O (data from Haas & Holdaway, 1973) for P_{total} = pH_2O (full lines) and for the lowest X_{H_2O} values in each group of samples (dotted line).

among groups can be seen. *Group 2* values are slightly higher than *Group 1* values, but *Group 3* values are well above the others. These data seem to be a direct consequence of the increasing proportion of the denser aqueous phase from *Group 1* to *Group 3*. In addition, the salinity is remarkably higher in *Group 3*. In spite of these variations, the true density cannot be determined for each group, as the fluid inclusions were apparently trapped from immiscible fluids. Only the variation as a function of different volumetric proportions (V_{CO_2}/V_{tot}) could be obtained, following the procedures discussed in Brown & Lamb (1986, 1989). These authors have shown that in fluid inclusion trapped below the immiscibility curve in the H_2O-CO_2 system, the true isochores should be located between those representing pure CO_2 and H_2O densities, considering by the volumetric proportions of these components. Apart from the small variations observed, the most noticeable features are the higher CO_2 content in inclusions of *Group 1* and *Group 2*, and the higher H_2O and NaCl molar fractions in inclusions of *Group 3*.

DISCUSSION

Data in tables I and II and the Th_{CO_2} histogram (Fig. 2) show only slight differences in their parameters when *Groups 1* and *2* are considered. In contrast, the *Group 3* inclusions show a clear difference in their values.

Apart from the inaccuracies due to difficulties in obtaining field relations, it seems to be clear that the differenciated characteristics of the mineralizing solutions of the three groups are in some way related to distinct inclusion trapping conditions and stages, and consequently to the host mineral crystallization. This behaviour may also be related to changes in the original inclusions due to post-cristallization events. However, only fluid inclusions with morphology indicative of primary and pseudosecondary origin without evidence of superimposed deformation were studied. Furthermore, there is some consistency in the measurements related to each group, even in a single sample, which supports the supposition that the first hypothesis is the most solid.

It should be also remarked that the small variations in a specific group are usually related to slightly different V_{CO_2}/V_{tot} values, which is directly related to the parameters obtained and to the observed types of total homogenization (critical, CO_2 expansion or CO_2 contraction). These behaviors are typical of inclusions trapped from an original immiscible fluid system (Roedder, 1984). Therefore, further to the slightly different trapping conditions and evolutive stages for the three groups, the aspects discussed above seem to indicate an originally heterogeneous fluid system composed predominantly by saline aqueous solutions and CO_2, with small amounts of N_2 and CH_4.

Roedder (1984) shows that the obtained temperature, pressure, and density from such systems are, in general, erroneous. However, in the present case, as the original solutions seem to have been trapped under conditions near the critical point, relatively narrow density ranges were obtained (Fig. 6). Therefore, the true densities of the mineralizing fluid should not be too far from the obtained limits in each group.

The determination of pressure for an originally heterogeneous system composed by aqueous saline solutions and CO_2, when the two components are trapped in different proportions, is relatively difficult (Roedder, 1984). However, knowing the approximate trapping temperatures, obtained from the lowest Th_{tot} values, and the d_{total} variation interval represented by their respective isochores, at least the extreme limits of the involved pressure can be obtained with some precision as discussed by Brown & Lamb (1986, 1989). Thus, considering the minimum Th_{tot} in the isochoric diagrams (Fig. 6), the following temperature and pressure intervals, have been determined:

Group 1: 290-300°C and 2.0 to 2.5kbar;

Group 2: 290-300°C and 2.1 to 2.8kbar;

Group 3: 275-285°C and 1.75 to 3.2kbar.

The isochores in figure 6, which indicated the mentioned P and T conditions, were determined using Bowers & Helgeson's (1983) equations for the H_2O-CO_2-NaCl system presented by Nichols & Crawford (1985). However, if the Brown & Lamb (1989) isochores are considered, the pressures ob-

tained are slightly higher, varying between 2.3 and 4.0kbar for the whole study.

The values presented above indicate that the inclusions of the three groups were trapped under slightly different T-P conditions, but still compatible with hydrothermal conditions, where the solutions percolating the host rocks may have been submitted to some compositional alterations.

In summary, it is suggested that aquo-carbonic hydrothermal fluids with low to moderate salinity (4.5-8.8wt% NaCl equiv.), 0.93 to 1.02g/cc total density, 275 to 300°C temperatures and 1.7 to 3.2kbar pressures, containing Be and F, account for the formation of euclase and topaz as well as other associated minerals.

Due to the presence of tremolite and pyrophyllite as crystalline inclusions in topaz the following reaction equilibrium curves were added in figure 6:

a) 5 dolomite + 8 quartz + H_2O = tremolite + 3 calcite + 7 CO_2, and

b) kaolinite + 2 quartz = pyrophyllite + H_2O,

considering the limits of variation of the calculated H_2O and CO_2 molar fractions for each group of samples, as seen in table II. Data for tremolite formation reaction were taken from Skippen (1974). The equilibrium curve for $X_{CO_2} = 0.03$ was obtained by graphic extrapolation.

The data for pyrophyllite reaction came from Haas & Holdaway (1973) for a Ptotal = pH_2O, with addition of the equilibrium curves for the lowest molar fractions of water vapor in inclusions of each group.

From figure 6 it can be deduced that the pyrophyllite and the tremolite, among other solid inclusion in the topaz, should precede the crystallization of the host, having been trapped during its growth. This may have occurred under post-metamorphic hydrothermal conditions probably linked to the last volcanism in the area, of upper Cretaceous or lower Terciary age as proposed by Ferreira (1983, 1991). The P and T conditions determined by the fluid inclusion studies are compatible with these conditions.

The decreasing CO_2 molar fraction towards *Group 3* inclusions (which also show the lower Th_{tot} values) suggests that they were formed later. This scenario is consistent with the expected evolution of the fluids. Nevertheless, the hypothesis considering that the X_{CO_2} variations may have been influenced by interactions between the mineralizing solutions and the host rocks with variable carbonate contents cannot be ruled out.

ACKNOWLEDGEMENTS

The authors would like to thank TIMCIL for supplying the samples; to CDTN/CNEN for the access to the fluid inclusion laboratory; to Prof. Dr. João Fernando Martins Hippertt, for the suggestions on the revision of the text, and to Luiz Raphael Aun, for drawing the figures. R. M. S. Bello and K. Fuzikawa acknowledge the CNPq support: processes 303872/85-3 and 300045/92-1, respectively; and J. V. Valarelli acknowledges the FAPESP support (process: 934811-8).

REFERENCES

ALKMIN, F. F.; QUADE, H. & EVANGELISTA, M. T. R., (s.d.), Sobre a história da deformação dos metassedimentos do Supergrupo Minas e Grupo Itacolomi no Quadrilátero Ferrífero, Minas Gerais. Publicação Interna UFOP, 45p.

BELLO, R. M. DA S.; GANDINI, A. L.; FUZIKAWA, K. & SVISERO, D. P., (1995), Estudo microtermométrico de inclusões fluidas do topázio imperial da jazida de Boa Vista, Ouro Preto, MG. *R. Esc. Minas*, Ouro Preto, **49** (2): 111-116.

BOWERS, T. S. & HELGESON, H. C., (1983), Calculation of the thermodynamic and geochemical consequences of nonideal mixing in the system H_2O-CO_2-NaCl on phase reactions in geologic systems: equation of state for H_2O-CO_2-NaCl fluids at high pressures and temperatures. *Geochim. Cosmochim. Acta,* **47:** 1247-1275.

BROWN, P. E. & LAMB, W. M., (1986), Mixing of H_2O-CO_2 in fluid inclusions; Geobarometry and Archean gold deposits. *Geochim. Cosmochim. Acta,* **50:** 847-852.

BROWN, P. E. & LAMB, W. M., (1989), P-V-T properties of fluids in the system $H_2O \pm CO_2 \pm NaCl$: New graphical presentations and implications for fluid inclusion studies. *Geochim. Cosmochim. Acta,* **53:** 1209-1221.

CASSEDANNE, J. P., (1989), Famous minerals localities: The Ouro Preto topaz mines. *Mineral. Rec.*, **20:** 221-233.

COLLINS, P. L. F., (1979), Gas hydrates in CO_2-bearing fluids and the use of freezing data for estimation of salinity. *Econ. Geol.*, **74** (6): 1435-1444.

FERREIRA, C. M., (1983), Vulcanismo ácido no Quadrilátero Ferrífero e sua relação com algumas ocorrências e/ou depósitos minerais. In: *Simpósio de Geologia de Minas Gerais*, 2. Belo Horizonte. Anais... Belo Horizonte, SBG, v. 3, p. 128-133.

FERREIRA, C. M., (1987), Geologia da jazida de topázio do Morro de Saramenha. *R. Esc. Minas*, Ouro Preto, **40** (3): 15-17.

FERREIRA, C. M., (1991), Topázio de Ouro Preto, Minas Gerais. *In*: SHOBBENHAUS, C.; QUEIROZ, E. T.; COELHO, C. E. S. Principais depósitos minerais do Brasil, vol IV, Parte A: *Gemas e Rochas Ornamentais*. Brasília, DNPM/CPRM, p. 303-308.

FUZIKAWA, K., (1985), Inclusões fluidas: métodos usuais de estudo e aplicações. *In*: SBG/CBMM, *Contribuições a Geologia e Petrologia*, Belo Horizonte, p. 29-44.

GANDINI, A. L., (1994), *Mineralogia, inclusões fluidas e aspectos genéticos do topázio imperial da região de Ouro Preto, Minas Gerais*. São Paulo. 212p. (Dissertação de Mestrado. Instituto de Geociências da USP).

GANDINI, A. L.; BELLO, R. M. DA S.; FUZIKAWA, K.; SVISERO, D. P. & FERREIRA, C. M., (1991), Caracterização das inclusões fluidas dos topázios imperiais da região de Ouro Preto, MG. *Bol. IG-USP, Ser. Cient.*, **22:** 61-72.

GANDINI, A. L.; MENDES, J. C. & SVISERO, D. P., (1992a), Dados mineralógicos preliminares de topázio imperial da região de Ouro Preto, Minas Gerais. In: *Congresso Brasileiro de Geologia*, 37, São Paulo. Boletim de Resumos Expandidos, v. 2, São Paulo, SBG, p. 110-111.

GANDINI, A. L.; BELLO, R. M. DA S.; FUZIKAWA, K.; MARCIANO, V. R. P. R. O.; PIMENTA, M. A. & SVISERO, D. P., (1992b), Microtermometria, absorção no infravermelho e espectroscopia micro Raman dos componentes químicos das inclusões fluidas dos topázios imperiais de Ouro Preto, MG. In: *Congresso Brasileiro de Geologia*, 37, São Paulo. Boletim de Resumos Expandidos, v. 2, São Paulo, SBG, p. 111-113.

GORCEIX, H., (1881), Estudo geológico das jazidas de topázio da Província de Minas Gerais, Brasil. *An. Esc. Min. Ouro Preto*, **1:** 13-34.

GÜBELIN, E.; GRAZIANI, G. & KAZMI, A. H., (1986), Pink topaz from Pakistan. *Gems and Gemology*, **22** (3): 141-151.

HAAS, H. & HOLDAWAY, M. J., (1973), Equilibria in the system Al_2O_3-SiO_2-H_2O involving the stability limits of pyrophyllite, and thermodynamic data of pyrophyllite. *Amer. Jour. Sci.*, **273:** 449-464.

MARSHAK, S. & ALKMIN, F. F., (1989), Proterozoic extension/contraction tectonics of the southern São Francisco Craton and adjacent regions, Minas Gerais, Brazil: a kinematic model relating Quadrilátero Ferrífero, São Francisco Basin and Cordilheira do Espinhaço. *Tectonics*, **8**(3): 555-571.

NICHOLLS, J. & CRAWFORD, M. L., (1985), Fortran programs for calculation of fluid properties from microthermometric data on fluid inclusions. *Geochim. Cosmochim. Acta*, **11** (5): 614-645.

OLSEN, D. R., (1971), Origin of topaz deposits near Ouro Preto, Minas Gerais, Brazil. *Econ. Geol.*, **66** (4): 627-631.

PETROV, I.; SCHMETZER, K. & BANK, H., (1977), Orangefarbene topaskristalle von Saramenha bei Ouro Preto, Minas Gerais, Brasilien. *Aufschluss*, **28:** 219-220.

PIRES, F. R. M., (1983), Geologia e gênese dos depósitos de topázio do Distrito de Ouro Preto – Minas Gerais. In: *Simpósio de Geologia de Minas Gerais*, 2, Belo Horizonte, 1983. Anais... Belo Horizonte, SBG, v. 3, p. 283-296.

POTY, B.; LEROY, J. & JACHIMOWICZ, L., (1976), Un nouvel appareil pour la mesure des températures sous le microscope: l'installation de microthermometrie CHAIXMECA. *Soc. Fr. Mineral. Cristallogr., Bull.*, **99** (2/3): 182-186.

ROEDDER, E., (1984), Fluid inclusions. *Reviews in Mineralogy*, **12:** 646p.

SKIPPEN, G., (1974), An experimental model for low pressure metamorphism of siliceous dolomitic marble. *Amer. Jour. Sci.*, **274:** 487-509.